Remote measurement of the 1992 Tapera prescribed fire at the Reserva Ecológica do IBGE

Philip J. Riggan, Robert G. Tissell, and Robert N. Lockwood

Introduction

Across the 2 million km^2 of the Cerrado ecosystem in central Brazil, open burnings of vegetation are a common and frequent disturbance. Their origins predominantly are human today, but evidence of frequent burnings extends millennia into records from lacustrine sediments (Ferraz-Vicentini 1999). Burning is a visible source of extensive particulate air pollution and likely an important source of carbon emissions to the atmosphere that may contribute to global climate change (Krug *et al.* 2006, Riggan *et al. in preparation*). The season and frequency of burning may have important ecological effects on the structure, composition, and persistence of natural vegetation (Sato *et al.* 1998). Many of the expected or realized ecological and atmospheric effects are likely related to fire intensity and the mass of biomass consumed, but because of the extreme environment of fires and the difficulty of approaching them, the physical nature and variability of burning has only recently been measured and appreciated.

Infrared light at wavelengths longer than 1.6 μm is transmitted with little attenuation through the smoke particulates that can obscure flames in visible wavelengths of light. Thus, remote sensing of emitted infrared light offers a means to obtain synoptic or wide-area measurements of fire properties, but most airborne or satellite-based sensors have been incapable of measuring the very high infrared radiances associated with wildland fires unless the signal is diluted by large areas of low-radiance background emissions, as with the Advanced Very High Resolution Radiometer (AVHRR) or the fire channel of the Moderate Resolution Imaging Spectroradiometers (MODIS), which have nominal resolution of 1 km.

Two airborne multi-spectral sensor systems have been specifically designed and deployed to quantitatively measure the radiances of wildland fires at high spatial resolution: these are an extended-dynamic-range imaging spectrometer (EDRIS), built by a partnership of the NASA Ames Research Center and the United States Forest Service, Pacific Southwest Research Station (PSW), and the FireMapper thermal-imaging radiometer, which was constructed through a research joint venture between PSW and Space Instruments, Inc. These instruments have been employed in central Brazil to make the first quantitative, high-resolution measurements of the thermal properties and radiant emissions of active wildland fires. Their application resulted from a multi-year effort led by the U.S. Forest Service and the Instituto Brasileiro do Meio Ambiente e dos Recursos Naturais Renováveis (IBAMA), through their Cooperation on Fire and Environmental Change in Tropical Ecosystems.

In this chapter we describe the results of remote sensing with EDRIS of a large prescribed fire and atmospheric measurements of its smoke plume in the Tapera area of the Reserva Ecológica of the Instituto Brasileiro de Geografia e Estatística at Brasília, DF, Brasil. To date this remains one of the best-documented burnings in tropical savanna.

Methodology

Setting of the 1992 Tapera fire

The Tapera fire was ignited by hand-carried drip torches within a watershed of low relief ranging from 1040 to 1130 m elevation. Ignition proceeded from south to north along the eastern margin of the experimental area, along a stream course on the north, and from east to west, keeping abreast of the spreading fire, along the south margin (Figure 1). The fire terminated at a constructed firebreak on the west. Plant communities were comprised of three physiognomies of the Cerrado – Campo Cerrado, Campo Sujo, and Campo Limpo – that were distributed in that order from higher to lower elevations. Biomass structure in these communities has been described by Ottmar *et al.* (2001). We made remote sensing or *in situ* plume measurements of the Tapera fire over approximately three-quarters of an hour from first ignition through the end of active combustion (Figures 1 and 2). Remote sensing passes were made in the direction of the ambient wind – which was from the east northeast – as indicated by the directional tilt of the generated smoke column.

Airborne measurement

Remote sensing and atmospheric measurements were made from a King Air B200t research aircraft operated by the U.S. National Center for Atmospheric Research (National Center for Atmospheric Research 1990). The aircraft alternately was flown for several passes at high altitude for remote sensing and through the upwelling smoke plume for atmospheric measurements near the ground. CO_2 mixing ratio was measured with a closed-path Licor model 6262 analyzer. The aircraft was also instrumented for fast-

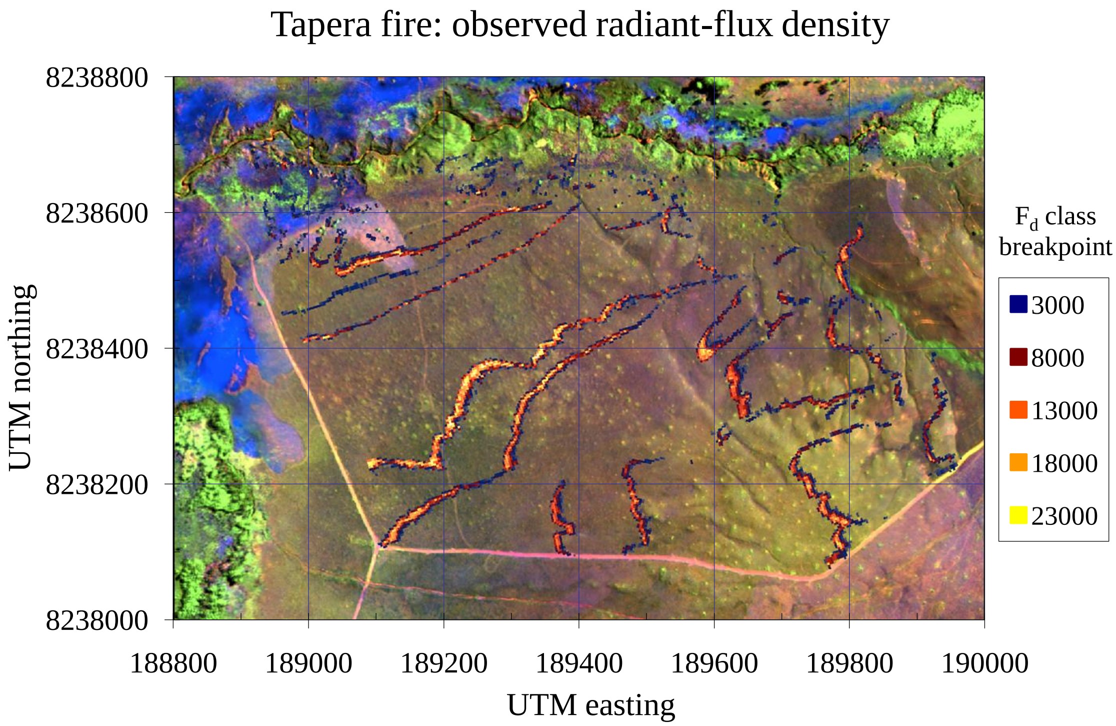

Figure 1. Observations of radiant-flux density (J m^{-2} s^{-1}) from six successive overflights of the 1992 Tapera fire. Fire-line data are depicted here on a multi-spectral image from the U.S. Forest Service's FireMapper remote-sensing system; the background image is constructed from reflected red light (mapped in red), reflected near-infrared light (mapped in green), and emitted thermal-infrared light mapped in blue. This scene from the year 2000 shows the structure of the vegetation in the fire area, roads and firebreaks in the vicinity, and areas that had recently burned along the gallery forest on the west and north and in campo at the southeast. Within the Tapera watershed are areas of campo limpo in reddish tones and campo rupestre in light green, such as just north of the bend in the southern road. Timing for successive fire observations is given in Figure 2. Note the substantial differences in radiant-flux density between adjacent fire runs near (189600, 8238400), between successive observations of the north line, and along the south line at 16:10 local time. In the latter case, active fire runs have merged into a line becoming more parallel with the wind; these runs maintain higher radiant-flux density than the trailing flanks.

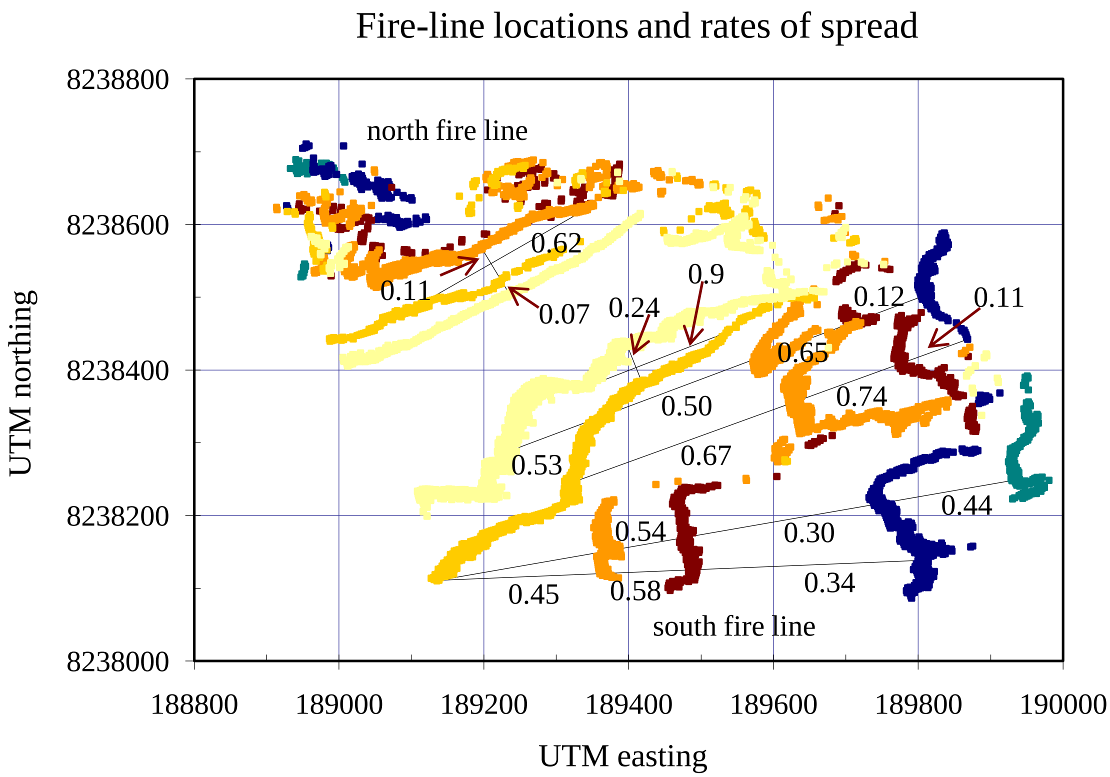

Figure 2. Progression map and rates of spread of the Tapera fire. Fire locations are color coded as follows: 15:35 local time (blue-green), 15:42 (dark blue), 15:58 (dark red), 16:01 (orange), 16:10 (gold), and 16:14 (yellow). Fire spread was generally from east-northeast to west southwest with the ambient wind. Ignition was primarily from upwind on the east and along a gallery forest on the north. Rates of spread along various vectors (shown as black lines) are indicated in m/s.

response measurement of atmospheric state variables and components of air velocity in three dimensions (Lenschow & Spyers-Duran 1989).

Remote-sensing methodology

Radiance of the Tapera fire was measured and its progression mapped by the EDRIS line scanner, which produces imagery at infrared wavelengths of 1.56 to 1.69 μm, 3.82 to 3.97 μm, and 11.5 to 12.2 μm with spatial resolution of 2.6 m per 1000 m of altitude above ground level (Riggan *et al.* 2004). These wavelength bands correspond to atmospheric windows in the infrared where radiation is not strongly absorbed by water vapor. The infrared channels of the spectrometer were calibrated in the laboratory over a target of high emissivity at temperatures ranging from 300 to 860 K. The instrument employed dual-range linear preamplifiers to allow measurements across a wide range of radiances.

Flame temperatures within a wildland fire can be estimated by an iterative solution of two instances of the Planck function – as given, for example, by Liou (1980) – using the radiance measured by high-resolution remote sensing at each of two infrared wavelengths (Riggan *et al.* 2004, Matson & Dozier 1981). We refer to this herein as the two-channel method. In this fashion estimation of temperature is independent of that for emissivity and the fractional area of the hot target within an observed pixel. Wavelengths near 1.6 and 3.9 µm are optimal for estimating flame temperatures since they fall on either side of the expected maximum in flame radiance (Riggan & Tissell 2009) and occur in atmospheric windows of high radiation transmittance.

The temperature and radiance at one wavelength then can be used to estimate the product of the bulk *emissivity* (ε) and the *fractional area* (A_f) of the hot target. Observed emissivity is likely a function of the high specific emissivity of soot particles entrained in flames and the low optical density of those particles. The fire's wavelength-integrated radiant-flux density, F_d (J m^{-2} s^{-1}), a measure of radiant fire intensity, can be estimated from flame temperature and the combined emissivity-fractional area as:

$$F_d = \varepsilon A_f \sigma T^4$$

where σ is the Stefan-Boltzmann constant, 5.67x10^{-8} J m^{-2} s^{-1} K^{-4}.

Model estimates for the leading edge of a Cerrado fire predict that hot ground and ash beneath a flaming front contribute approximately four percent of the radiance at 1.63 µm; three-fifths of the radiance at 3.9 µm, and nearly nine-tenths of the radiance at 11.9 µm (Riggan & Tissell 2009). High-temperature flames, in contrast, are expected to dominate radiant emissions at the shortest wavelength and provide two-fifths of the radiance at the intermediate wavelength. Because of the contribution from both flames and hot ash at 3.9 µm, application of the two-channel method employing radiances at 1.63 and 3.9 µm is expected to underestimate flame temperatures by approximately 60 K.

Fire observations

Flame temperatures and combined emissivity-fractional area estimated by the two-channel method

Flames in the Tapera fire were of high temperature – 95 percent of all fire-line observations were between 871 and 1469 K – but not bright compared with a classic blackbody radiator; 95 percent of these observations obtained values of εA_f between 0.006 and 0.250. (Temperature estimates associated with fire lines of the Tapera fire were rarely less than 800 K; we include here all observations greater than 700 K). Median observed temperature was 1101 K (828ºC); median observed εA_f was 0.049. Thus, observed fire lines had an expected brightness only five percent of that of a blackbody at equivalent temperature. We have previously observed a value of εA_f near unity only infrequently in high-resolution measurements of an intense fire in slashed tropical forest near Marabá (Riggan *et al*. 2004).

Mean flame temperatures varied little – from 1097 to 1125 K – across the six overflights of the Tapera fire. Mean temperature of all spatial observations was 1116 K (SD=165). Gradients in temperature were observed across the depth of fire lines, with highest temperatures generally measured at their leading edge (Figure 3). These gradients were not nearly as steep, however, as were the gradients in radiant-flux density. Time courses in temperature and radiant-flux density, estimated by applying to fire-line spatial data a time base derived from rate of spread, showed that temperatures along one fire run of 50 m width declined on average by approximately 300 K during 40 seconds of fire passage; radiant-flux density concurrently rose to a peak of approximately 12,000 J $m^{-2}s^{-1}$ after 9 seconds and fell to 2,300 within 40 seconds. Constructed trends in radiant-flux density with time were quite variable, which we suspect was likely a reflection of flame turbulence, and to some degree, spatial variations in fuel.

Radiant-flux density

Radiant-flux density apparently marked important variations in fire behavior in what was thought to be fairly uniform grassland fuels (Figure 1). The north fire line, which was largely oriented parallel to the ambient wind, overall showed a lower radiant-flux density than the south line, which especially during early to middle burning periods was more wind driven. The north line did wax and wane: segments therein developed higher radiant-flux density where small runs occurred at 16:01 local time; there were uniformly low values at 16:10; these had increased markedly by last observation at 16:14. Two adjacent fire runs on the south line near UTM coordinates 189600, 8238400 at 16:01 did exhibit markedly different levels of radiant-flux density, possibly due to differences

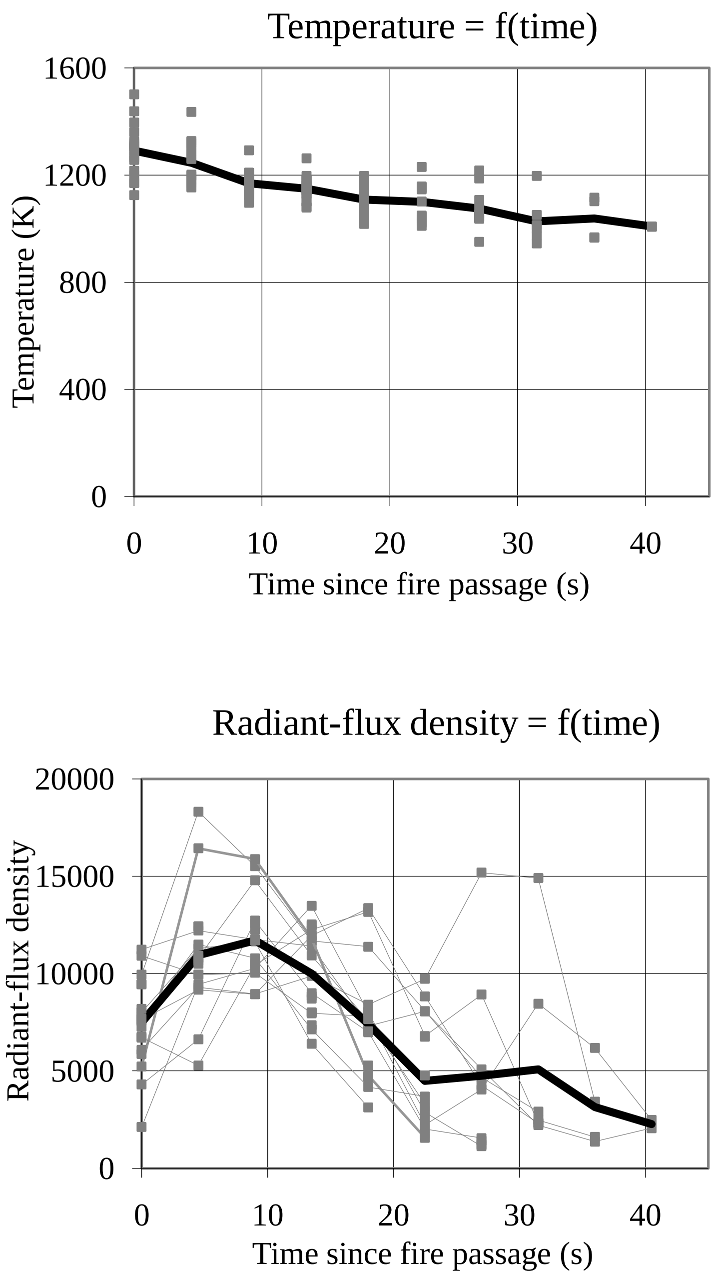

Figure 3. Estimated time courses, computed from rate of spread, in fire-line temperature (top) and radiant-flux density (bottom) along an approximately 50-meter-wide fire run as depicted at (189630, 8238350) in Figure 1. Averages are shown in the black line; individual samples along the fire line are shown in gray. Radiant-flux density declines more markedly over 40 seconds and is more highly variable than is fire-line temperature.

in fuels. These differences were not reflected in differences in flame temperature (from the two-channel method), but were apparent in the 11.9 μm radiometric temperature, which is thought to reflect the spatially averaged temperature of hot, high-emissivity ash beneath an active flaming zone. The south line at 16:10 local time was comprised of two regions of high radiant-flux density (Figure 4) – which appeared to correspond with extensions of earlier fire runs – each of which had associated trailing flanks of low radiant-flux density. These latter features in radiant-flux density were not present in the observed maximum fire-line temperatures (Figure 4) and appeared to result from variations in εA_f.

Another way to view the importance of observed distributions of temperature and εA_f is to examine the distribution of radiant-energy flux across these variables. Across all observations of the Tapera fire, ninety-five percent of the radiant-flux density was associated with temperatures between 898 and 1424 K and values of εA_f between 0.014 and 0.31 m^2/m^2. One half of the total radiant-flux density was observed at temperatures below 1131 K and a value of εA_f of 0.091. (These percentile values for all observations of the Tapera fire differ slightly from those previously reported by Riggan *et al*. (2004) for a single overflight of the fire.)

What is the relative importance of radiant-energy flux from high-temperature regions in a fire line as opposed to those of lower temperatures? The 4^{th} power dependence of radiant-flux density on temperature would appear to ascribe a *much* greater importance to relatively infrequent occurrences of high temperature. Observations show that this is not generally the case; the 20 percent of all observations

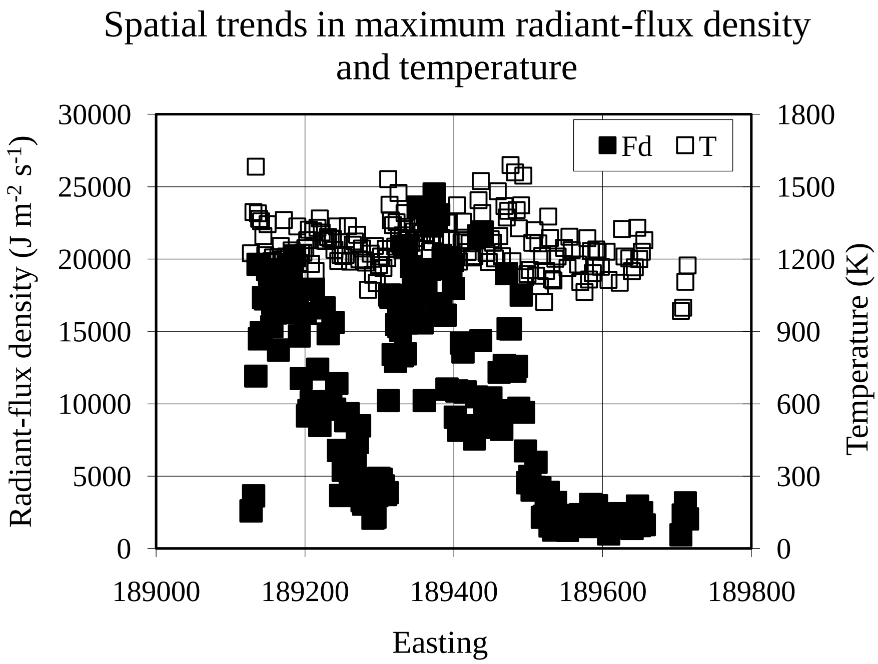

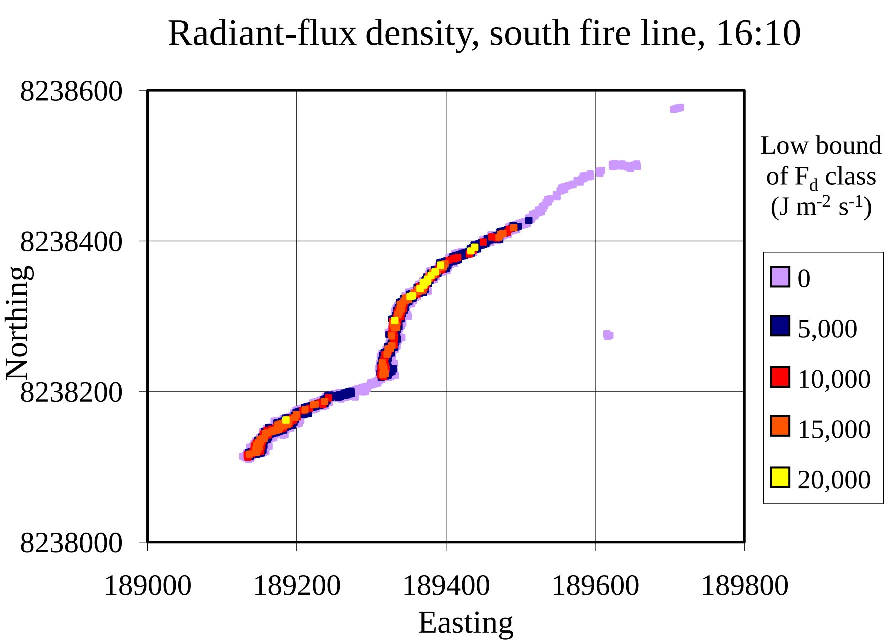

Figure 4. Trends in radiant-flux density, F_d, (J m^{-2} s^{-1}) and temperature, *T*, (K) (top) along the length of the south fire line at 16:10 (as shown at bottom). Note that although peak temperature along the length of the fire line shows seemingly random variation and no consistent trends, radiant-flux density clearly shows the inclusion of two energetic fire runs with trailing flanks of low intensity.

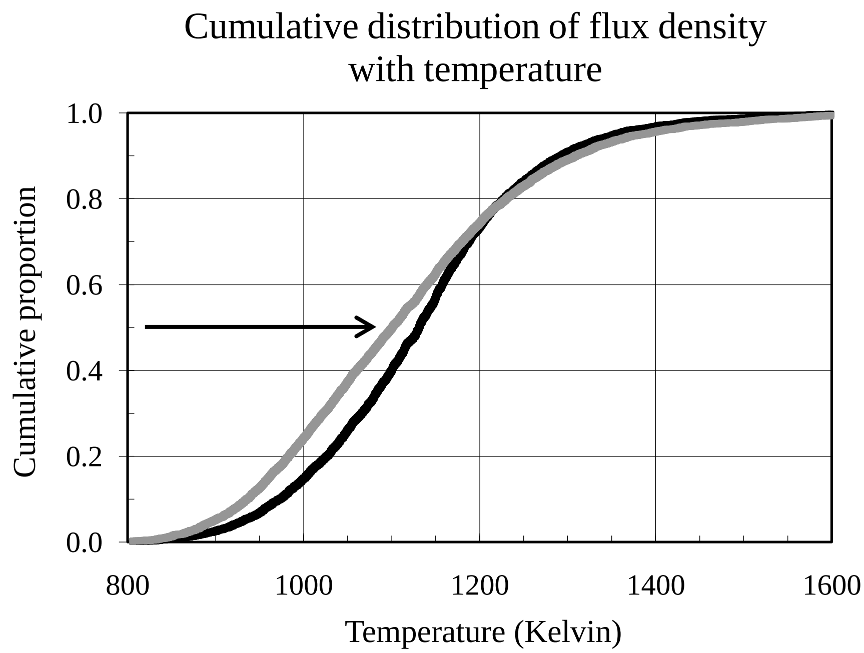

Figure 5. Cumulative distribution of flux density with temperature (dark symbols) compared with the cumulative distribution of all observations with temperature (gray symbols). The median value is marked by an arrow. Whereas one-half of all observations were associated with temperatures below 1101 K, these accounted for only 40 percent of the total radiant-flux density observed. Low temperature observations made a much less than proportional contribution to the overall radiant-flux density. Note that the 20 percent of all observations that were above 1230 K, accounted for an equivalent 20 percent of the total radiant-flux density.

of the Tapera fire that were above 1230 K, accounted for an equivalent 20 percent of the total radiant-flux density (Figure 5). Only at lower temperatures did the relative contribution to total radiant-flux density fall substantially in relation to the frequency of temperature occurrence: e.g., temperatures below 1000 K accounted for 24 percent of observations but only 15 percent of the flux density. These observations may be due in part to the decline in fractional area at the highest temperatures (Figure 6). This inverse relation may be due to the highest temperatures occurring at the leading edge of fire lines where fractional areas would be expected to be reduced or to a greater importance behind the fire's leading edge of background hot soil than flames; this would tend to increase

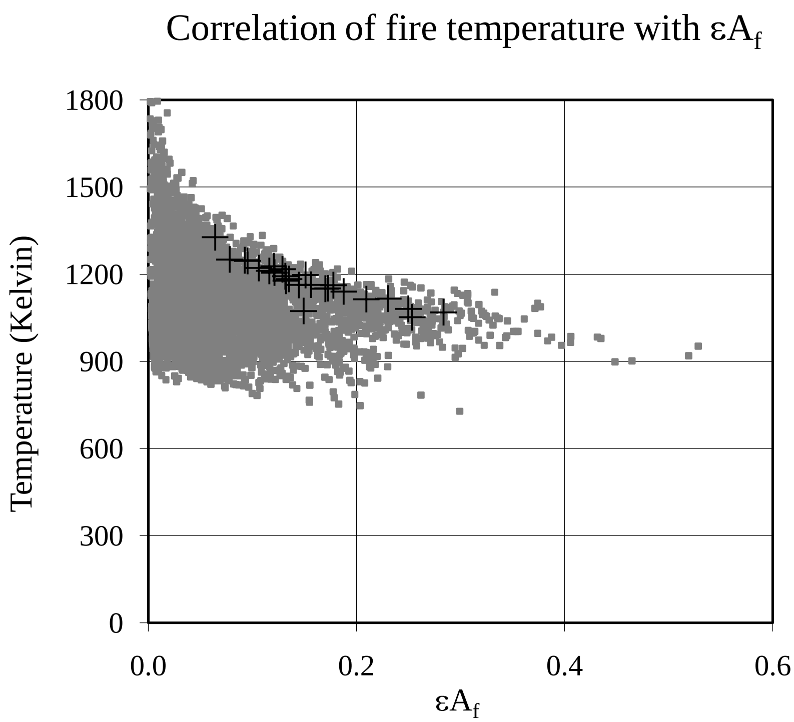

Figure 6. Distribution of temperature with emissivity-fractional area (εA_f) for all fire-line observations (gray symbols) and for a selection of pixels (as indicated by the + symbols) from a fire run at 16:01 local time (cf. Figure 3). Overall, εA_f was not a good predictor of fire temperatures, but in local areas of actively spreading fire there was an inverse relationship between the variables.

the apparent emissivity-fractional area while causing a relatively higher radiance at 3.9 µm compared with that at 1.6 µm, the effect of which would lead to a lower bulk temperature estimate by the two-channel method. Another possibility may be that the bulk emissivity of high temperature flames is reduced by lower soot-particle concentrations therein.

Measurements from both the Tapera fire in Cerrado vegetation and a fire in partially slashed tropical forest near Marabá showed that the radiant-flux density obtained from high-resolution radiance measurements at 1.63 and 3.9 µm could be predicted with high precision based on a linear relationship to the high-resolution measurement of fire radiance at 3.9 µm alone (Figure 7)(Riggan & Tissell 2009).

Why does this relationship exist? We note that the 3.9-µm wavelength is centrally located on a typical blackbody curve for the temperatures observed in wildland fires (cf. Riggan & Tissell 2009). A given value of radiant-flux density – the area under the Planck function – can be obtained by a range of conditions ranging from especially hot flames with low εA_f to cooler, yet hot, ground with high εA_f. For constant radiant-flux density and the observed range in flame temperatures, the above tradeoff results in only a small change in radiance at the central, 3.9-µm wavelength. The 1.6-µm radiance by contrast shows no such tradeoff and falls off markedly in the latter situation (very warm ground with high εA_f).

Rates of spread

As we have noted elsewhere (Riggan *et al. in preparation*) the rate of spread of a wildland fire may be problematic to quantify: what one observes with even frequent remote sensing is a semi-continuous, irregular line of the fire perimeter that is translated and stretched with time. For the Tapera Fire, the direction of spread from point to point was not readily identifiable, and even the rate of spread of the head of the fire was difficult to quantify because of the changing shape of the fire line – here we measured vectors of spread over a time interval without a point-to-point map of how the fire actually progressed. One can estimate directional components of the spread, for example along a particular azimuth or in the direction of the ambient wind, but these do not necessarily represent how the fire got from one point to another. The areal progression of

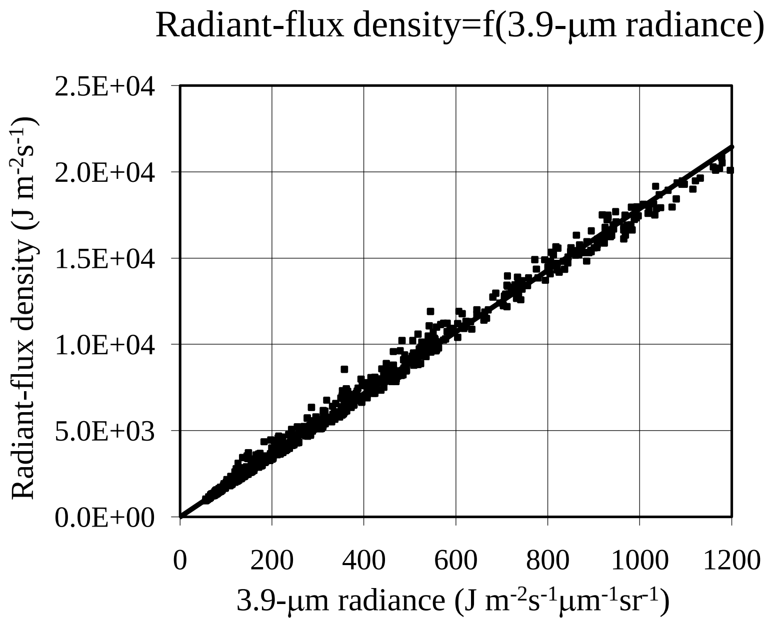

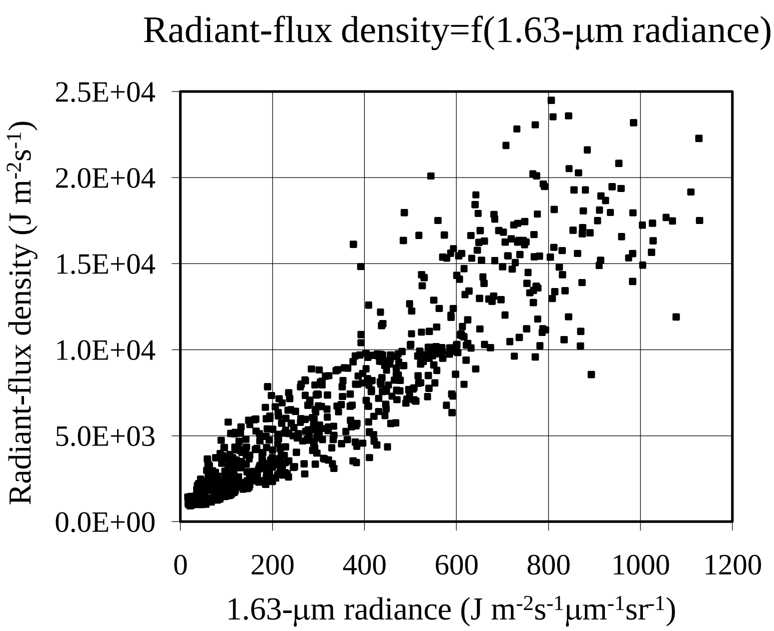

Figure 7. Radiant-flux density as a function of single-channel radiances for the Tapera fire. The 3.9-μm radiance (top) alone provides a good predictor of the radiant-flux density as determined by a two-channel method.

burning with time is better defined and more amenable to measurement.

Downwind spread of the Tapera Fire was marked by several nearly individual runs that remarkably did not progress together even with little variation in terrain or ignition timing (Figures 1 and 2). A run that developed from the earliest ignition in the southeast of the burned area was observed to spread initially at 0.44 m/s and throughout its course at from 0.3 to 0.58 m/s. The next segment ignited to the north initially bifurcated with each of two runs spreading at only 0.11 to 0.12 m/s. These quickly accelerated during the interval between the 3rd and 4th observations (from 15:58 to 16:01 local time) to spread at 0.65 to 0.74 m/s. We speculate that this high rate of spread may have been influenced by fire-generated winds associated with the southern-most, downwind fire run. By the 5th observation at 16:10 the second and third runs from the south had merged and begun to pivot, producing a fire line with a large component parallel to the ambient wind. Over this interval rates of spread consistently exceeded 0.5 m/s. None of the fire runs appeared to course the length of the planned burned area while maintaining a well-defined front perpendicular to the wind. Between the 5th and 6th observations, the trailing flank of the south line appeared to spread nearly perpendicular to the wind, but may have moved partially by a large and rapid translation largely along the line and in the direction of the ambient wind. Such a translation would have required a spread-rate vector of 0.9 m/s, somewhat above the upper range of observed values.

The north line of the Tapera Fire was ignited for fire control along the margin of a wetland area, which coincidentally was oriented parallel to the ambient wind. Over the first three observations burning there was not organized into a continuous line and observed radiant-flux density was low. At the 4th mapping of the fire at 16:01, approximately 26 minutes after first observation, the north line had become organized with two small lobes on the west and portions of the line with high values of radiant-flux density. Although overall the north line appeared to spread to the south-southeast, perpendicular to the wind, the high radiant-flux density at the 4^{th} mapping suggests a stronger directional component of spread with the wind and a small directional component uphill and perpendicular to the wind. In essence, the line may have propagated to the south-southeast by a strong translation nearly at a right angle to that direction and along its length. The apparent spread component with the wind there, 0.62 m/s, was within the realm of the rates observed for fire runs of the south fire line. We did observe from overhead that the flames of the north line generally were oriented with a tilt down the length of the fire line and not over the unburned fuel, thus one would not expect a large propagating flux perpendicular to the wind. By the 5^{th} mapping of the fire, 34 minutes after first observation, the north line had extended to the western end of the fire area and was oriented parallel to the ambient wind with low levels of radiant-flux density throughout its length. At last observation, the north line developed higher levels of radiant-flux density as it approached the south line.

Modeling fuel consumption and carbon flux to the atmosphere

Flame radiance and fire areal growth rate measured by remote sensing have provided a provisional but promising estimator for fuel consumption rate and the rates of carbon and sensible-heat flux to the atmosphere (Riggan *et al*. 2004).

Sensible-heat and carbon fluxes from three large fires in central Brazil, including the Tapera fire, were estimated from *in situ* aircraft-based measurements of smoke-plume cross-sectional area and the vertical components of wind velocity, air temperature, and CO_2 mixing ratio within those plumes. Carbon and energy flux per unit area burned were estimated for the Tapera fire from the ratio of these whole-fire rates and the associated areal progression of the fire over time (m^2/s) (Riggan *et al*. 2004). The plume-based fuel consumption estimate so derived, 1.1 kg/m^2, compared well with nearby ground-based estimates of biomass loss during burning in somewhat lighter fuels (0.8 to 1.0 kg/m^2) (Dias 1994).

Whole-plume carbon and sensible heat fluxes were then related to *remotely sensed* flame properties by a simple model. The model set the sensible-heat flux (Q_s) equal to the product of the density (ρ_{air}) and specific heat (C_p) of moist air, the eddy diffusivity of heat (K_H) – which was assumed proportional to flame temperature (T_f) – and the near-ground potential temperature gradient ($\partial\theta / \partial z$), which was taken as proportional to the difference between flame temperature and that of the overlying ambient air (T_{amb}). Thus, $Q_s = \rho_{air} C_p k_T T_f (T_f - T_{amb})$.

With Q_s given in J m^{-2} s^{-1}, ρ_{air} in g m^{-3}, C_p in J g^{-1} K^{-1}, and T in K, application of the model to remote-sensing observations of high-temperature ($T_f >$ 1100 K), flaming combustion of a fire in savanna vegetation yielded a value of the proportionality constant k_T = 0.0026. When applied to observations of a second free-burning savanna fire and of a tropical-forest slash fire, this remote-sensing-based model produced estimates of sensible heat flux that were highly consistent with *in situ* plume measurements from the two fires. Furthermore, whole-plume carbon flux was strongly correlated with the flux of sensible heat (Riggan *et al*. 2004). Thus, the rate of fuel consumption by flaming fronts of entire large fires could be estimated from fire *temperature* estimated from radiance at short- and mid-wave infrared wavelengths. It remains to be seen whether carbon and heat fluxes and plume rise can be as well related to the radiant-flux density or a single-wavelength fire radiance measurement.

Implications for large-scale fire monitoring

Wildland fires present a complex of thermal gradients comprised of flaming fronts, ash, residual flaming combustion, smoldering of larger biomass elements, and unburned vegetation (Riggan *et al.* 2004). Airborne remote sensing at high spatial-resolution provides an opportunity of resolving these components and gradients. Low-resolution observations, as with some satellite-based sensors such as the MODIS, will necessarily encompass radiation from a variety of these elements.

Based on these results, one would not expect a single mid-wave infrared channel at 3.9 µm, as measured by MODIS, to adequately represent the diversity of temperatures and low εA_f occurring in nature. Furthermore, one could not estimate both temperature and εA_f from such a single item of information, and neither temperature nor εA_f were constant even across savanna fires with a limited range in fuel loading. Direct knowledge of fire temperatures may be important for understanding some fire effects; for example, in one large cerrado fire large reaches of low temperature, residual combustion were associated with high rates of carbon monoxide and methane emissions (Riggan *et al.* 2004). However, as shown above, the radiant-flux density *could be predicted with high precision* based on a linear relationship to the high-resolution measurement of fire radiance at 3.9 µm alone. Furthermore, ignoring the "background" radiance, an *average*

3.9 µm radiance from across a coarse-resolution pixel might be expected to adequately estimate an *average* radiant-flux density for the incorporated high-temperature elements. Thus, a single channel of MODIS data, absent considerations of background non-fire radiance within a pixel, might adequately represent the average radiant-flux density as measured at high resolution. However, the problematic nature of correcting for background radiance may obfuscate the measurement of fire intensity. Given the above considerations, a rigorous test is needed to examine the adequacy of coarse-resolution satellite-based observations, such as the MODIS 3.96 µm fire channel, as a means to extensively measure fire properties including radiant-flux density and estimate emissions to the atmosphere.

Conclusions

Remote measurements of the Tapera fire have provided an unprecedented look at the physical properties of a free-burning wildland fire. Although the *mean* radiometric temperature, determined from radiances at 1.6 and 3.9 µm, varied only by 128 K across six successive overflights, spatial variation in temperature was much greater: 95 percent of all spatial measurements spanned a range of ca. 600 K (from 871 to 1469 K). Much of this variation appeared to be associated with gradients across the width of fire lines. Emissivity-fractional area of the fire attained only low values overall, thus, at short- and mid-wave infrared wavelengths the fire was not especially bright in comparison to a blackbody radiator. In comparison with fire-line temperature, radiant-flux density, which is a measure of fire intensity, showed greater variability from regions of actively spreading fire lines to the fire’s trailing flank and across the width of some actively spreading fire runs. Fire was observed to spread along vectors with the wind at velocities of up to 0.74 m/s. Several individual fire runs that developed early in the burning period coalesced into a single line that pivoted to run more parallel to the wind. Some reaches of apparently slow lateral spread of the fire perpendicular to the wind may have been due to a rapid translation of the line nearly down its length. Fire radiant-flux density was well correlated with the measured radiance of the fire at 3.9-µm wavelength; measurements at that single wavelength could be used to map important features of fire behavior. Remote sensing methodology first applied at the Tapera fire is expected to have wide application for understanding the behavior and environmental effects of wildland fires.

Acknowledgements

We wish to acknowledge support for this research by the Instituto Brasileiro do Meio Ambiente e dos Recursos Naturais Renováveis; the USDA Forest Service, International Programs and Global Change Research Program; the U.S. Agency for International Development, Global Change Program; the USDA Foreign Agricultural Service, Research and Scientific Exchange Division; the NASA Process Studies Program; the National Center for Atmospheric Research; and the Instituto Brasileiro de Geographia e Estatística. For their important contributions we wish to thank Heloisa S. Miranda, João Antonio Raposo Pereira, Braulio Dias, Antônio Miranda, James Brass, Robert Higgins, Ted Hildum, Larry Radke, and Lynn Wolden.

Literature cited

DIAS, I. F. O. **Efeitos da queima no regime térmico do solo e na produção primária de um campo sujo de cerrado.** 1994. Dissertação de Mestrado. Departamento de Ecologia. Universidade de Brasília, Brasília.

FERRAZ-VICENTINI, K. R. C. **História do fogo no Cerrado.** Tese de Doutorado. Universidade de Brasília. Brasília, 1999.

KRUG, T.; FIGUEIREDO, H. B.; SANO, E. E.; ALMEIDA, C. A.; SANTOS, J. R.; MIRANDA, H. S.; SATO, M. N.; AND ANDRADE, S. M. A. 2006. **Primeiro Inventário Brasileiro de Emissões Antrópica de Gases de Efeito Estufa Relatórios de Referência Emissões de Gases de Efeito Estufa da Queima de Biomassa no Cerrado Não-Antrópico Utilizando Dados Orbitais.** Ministério da Ciência e Tecnologia, 2006. Available online at ‹http://www.mct.gov.br/upd_blob/0008/8805.pdf›.

LENSCHOW, D. H. & SPYERS-DURAN, P. **Measurement Techniques: Air Motion Sensing.** National Center for Atmospheric Research, Research Aviation Facility, 1989. Boulder, Colorado, USA. (Bulletin 23).

LIOU, K. ***An introduction to atmospheric radiation.*** London, England. Academic Press, 1980. International Geophysics Series, vol. 26, London, England.

MATSON, M. & DOZIER, J. **Identification of subresolution high temperature sources using a thermal IR sensor.** *Photogrammetric Engineering and Remote Sensing*, 47:1311-1318. 1981.

NATIONAL CENTER FOR ATMOSPHERIC RESEARCH. **The King Air: Overview and Summary of Capabilities. National Center for Atmospheric Research, Research Aviation Facility**, Bulletin 2, Boulder, Colorado, USA. 1990.

OTTMAR, R. D.; VIHNANEK, R. E.; MIRANDA, H. S.; SATO, M. N.; & ANDRADE, S. M. A. **Stereo photo series for quantifying Cerrado fuels in Central Brazil.** 2001. Vol. 1. General Technical Report PNW-GTR-519. Portland, Oregon: United States Department of Agriculture, Forest Service, Pacific Northwest Research Station.

RIGGAN, P. J. & TISSELL, R. G. **Airborne remote sensing of wildland fires,** In: *Wildland Fires and Air Pollution.* A. Bytnerowicz; M. Arbaugh; A. Riebau & C. Andersen (eds.). 2009. Vol. 8, Developments in Environmental Science, Elsevier Publishers, Amsterdam, The Netherlands. pp.139-170.

RIGGAN, P. J.; LOCKWOOD, R. N.; TISSELL, R. G.; BRASS, J. A.; PEREIRA, J. A. R.; MIRANDA, H. S.; MIRANDA, A. C.; CAMPOS, T.; AND HIGGINS, R. **Remote measurement of energy and carbon flux from wildfires in Brazil**. *Ecological Applications*, 14(3):855-872. 2004.

RIGGAN, P. J.; WOLDEN, L. G.; RECHEL, J.; TISSELL, R. G.; MIRANDA, H. S.; PEREIRA, J. A. R.; & BRASS, J. A. **Fire occurrence and carbon emission from burning in the Brazilian Cerrado ecosystem**. *In preparation*.

SATO, M. N.; GARDA, A. A.; & MIRANDA, H. S. **Effects of fire on the mortality of woody vegetation in central Brazil.** In: *Proceedings of the 3rd International Conference on Forest Fire Research and 14th Conference on Fire and Forest Meteorology*. D. X. Viegas (ed.). 1998. Vol. II, ADAI, University of Coimbra, Portugal. pp. 1777-1784.